

Search for the Decay $B^0 \rightarrow \rho^0 \rho^0$

The *BABAR* Collaboration

August 13, 2004

Abstract

The $B^0 \rightarrow \rho^0 \rho^0$ decay mode is searched for in a data sample of about 227 million $\Upsilon(4S) \rightarrow B\bar{B}$ decays collected with the *BABAR* detector at the PEP-II asymmetric B factory at SLAC. No significant signal is observed, and an upper limit of 1.1×10^{-6} (90% C.L.) on the branching fraction is set. Implications on the penguin contribution and constraints on the CKM angle α with $B \rightarrow \rho\rho$ decays are discussed. All results are preliminary.

Submitted to the 32nd International Conference on High-Energy Physics, ICHEP 04,
16 August—22 August 2004, Beijing, China

Stanford Linear Accelerator Center, Stanford University, Stanford, CA 94309

Work supported in part by Department of Energy contract DE-AC03-76SF00515.

The BABAR Collaboration,

B. Aubert, R. Barate, D. Boutigny, F. Couderc, J.-M. Gaillard, A. Hicheur, Y. Karyotakis, J. P. Lees,
V. Tisserand, A. Zghiche

Laboratoire de Physique des Particules, F-74941 Annecy-le-Vieux, France

A. Palano, A. Pompili

Università di Bari, Dipartimento di Fisica and INFN, I-70126 Bari, Italy

J. C. Chen, N. D. Qi, G. Rong, P. Wang, Y. S. Zhu

Institute of High Energy Physics, Beijing 100039, China

G. Eigen, I. Ofte, B. Stugu

University of Bergen, Inst. of Physics, N-5007 Bergen, Norway

G. S. Abrams, A. W. Borgland, A. B. Breon, D. N. Brown, J. Button-Shafer, R. N. Cahn, E. Charles,
C. T. Day, M. S. Gill, A. V. Gritsan, Y. Groysman, R. G. Jacobsen, R. W. Kadel, J. Kadyk, L. T. Kerth,
Yu. G. Kolomensky, G. Kukartsev, G. Lynch, L. M. Mir, P. J. Oddone, T. J. Orimoto, M. Pripstein,
N. A. Roe, M. T. Ronan, V. G. Shelkov, W. A. Wenzel

Lawrence Berkeley National Laboratory and University of California, Berkeley, CA 94720, USA

M. Barrett, K. E. Ford, T. J. Harrison, A. J. Hart, C. M. Hawkes, S. E. Morgan, A. T. Watson

University of Birmingham, Birmingham, B15 2TT, United Kingdom

M. Fritsch, K. Goetzen, T. Held, H. Koch, B. Lewandowski, M. Pelizaeus, M. Steinke
Ruhr Universität Bochum, Institut für Experimentalphysik 1, D-44780 Bochum, Germany

J. T. Boyd, N. Chevalier, W. N. Cottingham, M. P. Kelly, T. E. Latham, F. F. Wilson

University of Bristol, Bristol BS8 1TL, United Kingdom

T. Cuhadar-Donszelmann, C. Hearty, N. S. Knecht, T. S. Mattison, J. A. McKenna, D. Thiessen

University of British Columbia, Vancouver, BC, Canada V6T 1Z1

A. Khan, P. Kyberd, L. Teodorescu

Brunel University, Uxbridge, Middlesex UB8 3PH, United Kingdom

A. E. Blinov, V. E. Blinov, V. P. Druzhinin, V. B. Golubev, V. N. Ivanchenko, E. A. Kravchenko,
A. P. Onuchin, S. I. Serebnyakov, Yu. I. Skovpen, E. P. Solodov, A. N. Yushkov

Budker Institute of Nuclear Physics, Novosibirsk 630090, Russia

D. Best, M. Bruinsma, M. Chao, I. Eschrich, D. Kirkby, A. J. Lankford, M. Mandelkern, R. K. Mommsen,
W. Roethel, D. P. Stoker

University of California at Irvine, Irvine, CA 92697, USA

C. Buchanan, B. L. Hartfiel

University of California at Los Angeles, Los Angeles, CA 90024, USA

S. D. Foulkes, J. W. Gary, B. C. Shen, K. Wang

University of California at Riverside, Riverside, CA 92521, USA

- D. del Re, H. K. Hadavand, E. J. Hill, D. B. MacFarlane, H. P. Paar, Sh. Rahatlou, V. Sharma
University of California at San Diego, La Jolla, CA 92093, USA
- J. W. Berryhill, C. Campagnari, B. Dahmes, O. Long, A. Lu, M. A. Mazur, J. D. Richman, W. Verkerke
University of California at Santa Barbara, Santa Barbara, CA 93106, USA
- T. W. Beck, A. M. Eisner, C. A. Heusch, J. Kroseberg, W. S. Lockman, G. Nesom, T. Schalk,
B. A. Schumm, A. Seiden, P. Spradlin, D. C. Williams, M. G. Wilson
University of California at Santa Cruz, Institute for Particle Physics, Santa Cruz, CA 95064, USA
- J. Albert, E. Chen, G. P. Dubois-Felsmann, A. Dvoretzskii, D. G. Hitlin, I. Narsky, T. Piatenko,
F. C. Porter, A. Ryd, A. Samuel, S. Yang
California Institute of Technology, Pasadena, CA 91125, USA
- S. Jayatileke, G. Mancinelli, B. T. Meadows, M. D. Sokoloff
University of Cincinnati, Cincinnati, OH 45221, USA
- T. Abe, F. Blanc, P. Bloom, S. Chen, W. T. Ford, U. Nauenberg, A. Olivas, P. Rankin, J. G. Smith,
J. Zhang, L. Zhang
University of Colorado, Boulder, CO 80309, USA
- A. Chen, J. L. Harton, A. Soffer, W. H. Toki, R. J. Wilson, Q. Zeng
Colorado State University, Fort Collins, CO 80523, USA
- D. Altenburg, T. Brandt, J. Brose, M. Dickopp, E. Feltresi, A. Hauke, H. M. Lacker, R. Müller-Pfefferkorn,
R. Nogowski, S. Otto, A. Petzold, J. Schubert, K. R. Schubert, R. Schwierz, B. Spaan, J. E. Sundermann
Technische Universität Dresden, Institut für Kern- und Teilchenphysik, D-01062 Dresden, Germany
- D. Bernard, G. R. Bonneaud, F. Brochard, P. Grenier, S. Schrenk, Ch. Thiebaux, G. Vasileiadis, M. Verderi
Ecole Polytechnique, LLR, F-91128 Palaiseau, France
- D. J. Bard, P. J. Clark, D. Lavin, F. Muheim, S. Playfer, Y. Xie
University of Edinburgh, Edinburgh EH9 3JZ, United Kingdom
- M. Andreotti, V. Azzolini, D. Bettoni, C. Bozzi, R. Calabrese, G. Cibinetto, E. Luppi, M. Negrini,
L. Piemontese, A. Sarti
Università di Ferrara, Dipartimento di Fisica and INFN, I-44100 Ferrara, Italy
- E. Treadwell
Florida A&M University, Tallahassee, FL 32307, USA
- F. Anulli, R. Baldini-Ferroli, A. Calcaterra, R. de Sangro, G. Finocchiaro, P. Patteri, I. M. Peruzzi,
M. Piccolo, A. Zallo
Laboratori Nazionali di Frascati dell'INFN, I-00044 Frascati, Italy
- A. Buzzo, R. Capra, R. Contri, G. Crosetti, M. Lo Vetere, M. Macri, M. R. Monge, S. Passaggio,
C. Patrignani, E. Robutti, A. Santroni, S. Tosi
Università di Genova, Dipartimento di Fisica and INFN, I-16146 Genova, Italy
- S. Bailey, G. Brandenburg, K. S. Chaisanguanthum, M. Morii, E. Won
Harvard University, Cambridge, MA 02138, USA

R. S. Dubitzky, U. Langenegger

Universität Heidelberg, Physikalisches Institut, Philosophenweg 12, D-69120 Heidelberg, Germany

W. Bhimji, D. A. Bowerman, P. D. Dauncey, U. Egede, J. R. Gaillard, G. W. Morton, J. A. Nash,
M. B. Nikolich, G. P. Taylor

Imperial College London, London, SW7 2AZ, United Kingdom

M. J. Charles, G. J. Grenier, U. Mallik

University of Iowa, Iowa City, IA 52242, USA

J. Cochran, H. B. Crawley, J. Lamsa, W. T. Meyer, S. Prell, E. I. Rosenberg, A. E. Rubin, J. Yi

Iowa State University, Ames, IA 50011-3160, USA

M. Biasini, R. Covarelli, M. Pioppi

Università di Perugia, Dipartimento di Fisica and INFN, I-06100 Perugia, Italy

M. Davier, X. Giroux, G. Grosdidier, A. Höcker, S. Laplace, F. Le Diberder, V. Lepeltier, A. M. Lutz,
T. C. Petersen, S. Plaszczynski, M. H. Schune, L. Tantot, G. Wormser

Laboratoire de l'Accélérateur Linéaire, F-91898 Orsay, France

C. H. Cheng, D. J. Lange, M. C. Simani, D. M. Wright

Lawrence Livermore National Laboratory, Livermore, CA 94550, USA

A. J. Bevan, C. A. Chavez, J. P. Coleman, I. J. Forster, J. R. Fry, E. Gabathuler, R. Gamet,
D. E. Hutchcroft, R. J. Parry, D. J. Payne, R. J. Sloane, C. Touramanis

University of Liverpool, Liverpool L69 7ZE, United Kingdom

J. J. Back,¹ C. M. Cormack, P. F. Harrison,¹ F. Di Lodovico, G. B. Mohanty¹

Queen Mary, University of London, E1 4NS, United Kingdom

C. L. Brown, G. Cowan, R. L. Flack, H. U. Flaecher, M. G. Green, P. S. Jackson, T. R. McMahon,
S. Ricciardi, F. Salvatore, M. A. Winter

*University of London, Royal Holloway and Bedford New College, Egham, Surrey TW20 0EX,
United Kingdom*

D. Brown, C. L. Davis

University of Louisville, Louisville, KY 40292, USA

J. Allison, N. R. Barlow, R. J. Barlow, P. A. Hart, M. C. Hodgkinson, G. D. Lafferty, A. J. Lyon,
J. C. Williams

University of Manchester, Manchester M13 9PL, United Kingdom

A. Farbin, W. D. Hulsbergen, A. Jawahery, D. Kovalskyi, C. K. Lae, V. Lillard, D. A. Roberts

University of Maryland, College Park, MD 20742, USA

G. Blaylock, C. Dallapiccola, K. T. Flood, S. S. Hertzbach, R. Kofler, V. B. Koptchev, T. B. Moore,
S. Saremi, H. Staengle, S. Willocq

University of Massachusetts, Amherst, MA 01003, USA

¹Now at Department of Physics, University of Warwick, Coventry, United Kingdom

R. Cowan, G. Sciolla, S. J. Sekula, F. Taylor, R. K. Yamamoto
Massachusetts Institute of Technology, Laboratory for Nuclear Science, Cambridge, MA 02139, USA

D. J. J. Mangeol, P. M. Patel, S. H. Robertson
McGill University, Montréal, QC, Canada H3A 2T8

A. Lazzaro, V. Lombardo, F. Palombo
Università di Milano, Dipartimento di Fisica and INFN, I-20133 Milano, Italy

J. M. Bauer, L. Cremaldi, V. Eschenburg, R. Godang, R. Kroeger, J. Reidy, D. A. Sanders, D. J. Summers,
H. W. Zhao
University of Mississippi, University, MS 38677, USA

S. Brunet, D. Côté, P. Taras
Université de Montréal, Laboratoire René J. A. Lévesque, Montréal, QC, Canada H3C 3J7

H. Nicholson
Mount Holyoke College, South Hadley, MA 01075, USA

N. Cavallo,² F. Fabozzi,² C. Gatto, L. Lista, D. Monorchio, P. Paolucci, D. Piccolo, C. Sciacca
Università di Napoli Federico II, Dipartimento di Scienze Fisiche and INFN, I-80126, Napoli, Italy

M. Baak, H. Bulten, G. Raven, H. L. Snoek, L. Wilden
*NIKHEF, National Institute for Nuclear Physics and High Energy Physics, NL-1009 DB Amsterdam,
The Netherlands*

C. P. Jessop, J. M. LoSecco
University of Notre Dame, Notre Dame, IN 46556, USA

T. Allmendinger, K. K. Gan, K. Honscheid, D. Hufnagel, H. Kagan, R. Kass, T. Pulliam, A. M. Rahimi,
R. Ter-Antonyan, Q. K. Wong
Ohio State University, Columbus, OH 43210, USA

J. Brau, R. Frey, O. Igonkina, C. T. Potter, N. B. Sinev, D. Strom, E. Torrence
University of Oregon, Eugene, OR 97403, USA

F. Colecchia, A. Dorigo, F. Galeazzi, M. Margoni, M. Morandin, M. Posocco, M. Rotondo, F. Simonetto,
R. Stroili, G. Tiozzo, C. Voci
Università di Padova, Dipartimento di Fisica and INFN, I-35131 Padova, Italy

M. Benayoun, H. Briand, J. Chauveau, P. David, Ch. de la Vaissière, L. Del Buono, O. Hamon,
M. J. J. John, Ph. Leruste, J. Malcles, J. Ocariz, M. Pivk, L. Roos, S. T'Jampens, G. Therin
*Universités Paris VI et VII, Laboratoire de Physique Nucléaire et de Hautes Energies, F-75252 Paris,
France*

P. F. Manfredi, V. Re
Università di Pavia, Dipartimento di Elettronica and INFN, I-27100 Pavia, Italy

²Also with Università della Basilicata, Potenza, Italy

P. K. Behera, L. Gladney, Q. H. Guo, J. Panetta
University of Pennsylvania, Philadelphia, PA 19104, USA

C. Angelini, G. Batignani, S. Bettarini, M. Bondioli, F. Bucci, G. Calderini, M. Carpinelli, F. Forti,
M. A. Giorgi, A. Lusiani, G. Marchiori, F. Martinez-Vidal,³ M. Morganti, N. Neri, E. Paoloni, M. Rama,
G. Rizzo, F. Sandrelli, J. Walsh
Università di Pisa, Dipartimento di Fisica, Scuola Normale Superiore and INFN, I-56127 Pisa, Italy

M. Haire, D. Judd, K. Paick, D. E. Wagoner
Prairie View A&M University, Prairie View, TX 77446, USA

N. Danielson, P. Elmer, Y. P. Lau, C. Lu, V. Miftakov, J. Olsen, A. J. S. Smith, A. V. Telnov
Princeton University, Princeton, NJ 08544, USA

F. Bellini, G. Cavoto,⁴ R. Faccini, F. Ferrarotto, F. Ferroni, M. Gaspero, L. Li Gioi, M. A. Mazzoni,
S. Morganti, M. Pierini, G. Piredda, F. Safai Tehrani, C. Voena
Università di Roma La Sapienza, Dipartimento di Fisica and INFN, I-00185 Roma, Italy

S. Christ, G. Wagner, R. Waldi
Universität Rostock, D-18051 Rostock, Germany

T. Adye, N. De Groot, B. Franek, N. I. Geddes, G. P. Gopal, E. O. Olaiya
Rutherford Appleton Laboratory, Chilton, Didcot, Oxon, OX11 0QX, United Kingdom

R. Aleksan, S. Emery, A. Gaidot, S. F. Ganzhur, P.-F. Giraud, G. Hamel de Monchenault, W. Kozanecki,
M. Legendre, G. W. London, B. Mayer, G. Schott, G. Vasseur, Ch. Yèche, M. Zito
DSM/Daphnia, CEA/Saclay, F-91191 Gif-sur-Yvette, France

M. V. Purohit, A. W. Weidemann, J. R. Wilson, F. X. Yumiceva
University of South Carolina, Columbia, SC 29208, USA

D. Aston, R. Bartoldus, N. Berger, A. M. Boyarski, O. L. Buchmueller, R. Claus, M. R. Convery,
M. Cristinziani, G. De Nardo, D. Dong, J. Dorfan, D. Dujmic, W. Dunwoodie, E. E. Elsen, S. Fan,
R. C. Field, T. Glanzman, S. J. Gowdy, T. Hadig, V. Halyo, C. Hast, T. Hryn'ova, W. R. Innes,
M. H. Kelsey, P. Kim, M. L. Kocian, D. W. G. S. Leith, J. Libby, S. Luitz, V. Luth, H. L. Lynch,
H. Marsiske, R. Messner, D. R. Muller, C. P. O'Grady, V. E. Ozcan, A. Perazzo, M. Perl, S. Petrak,
B. N. Ratcliff, A. Roodman, A. A. Salnikov, R. H. Schindler, J. Schwiening, G. Simi, A. Snyder, A. Soha,
J. Stelzer, D. Su, M. K. Sullivan, J. Va'vra, S. R. Wagner, M. Weaver, A. J. R. Weinstein,
W. J. Wisniewski, M. Wittgen, D. H. Wright, A. K. Yarritu, C. C. Young
Stanford Linear Accelerator Center, Stanford, CA 94309, USA

P. R. Burchat, A. J. Edwards, T. I. Meyer, B. A. Petersen, C. Roat
Stanford University, Stanford, CA 94305-4060, USA

S. Ahmed, M. S. Alam, J. A. Ernst, M. A. Saeed, M. Saleem, F. R. Wappler
State University of New York, Albany, NY 12222, USA

³Also with IFIC, Instituto de Física Corpuscular, CSIC-Universidad de Valencia, Valencia, Spain

⁴Also with Princeton University, Princeton, USA

W. Bugg, M. Krishnamurthy, S. M. Spanier
University of Tennessee, Knoxville, TN 37996, USA

R. Eckmann, H. Kim, J. L. Ritchie, A. Satpathy, R. F. Schwitters
University of Texas at Austin, Austin, TX 78712, USA

J. M. Izen, I. Kitayama, X. C. Lou, S. Ye
University of Texas at Dallas, Richardson, TX 75083, USA

F. Bianchi, M. Bona, F. Gallo, D. Gamba
Università di Torino, Dipartimento di Fisica Sperimentale and INFN, I-10125 Torino, Italy

L. Bosisio, C. Cartaro, F. Cossutti, G. Della Ricca, S. Dittongo, S. Grancagnolo, L. Lanceri, P. Poropat,⁵
L. Vitale, G. Vuagnin
Università di Trieste, Dipartimento di Fisica and INFN, I-34127 Trieste, Italy

R. S. Panvini
Vanderbilt University, Nashville, TN 37235, USA

Sw. Banerjee, C. M. Brown, D. Fortin, P. D. Jackson, R. Kowalewski, J. M. Roney, R. J. Sobie
University of Victoria, Victoria, BC, Canada V8W 3P6

H. R. Band, B. Cheng, S. Dasu, M. Datta, A. M. Eichenbaum, M. Graham, J. J. Hollar, J. R. Johnson,
P. E. Kutter, H. Li, R. Liu, A. Mihalyi, A. K. Mohapatra, Y. Pan, R. Prepost, P. Tan, J. H. von
Wimmersperg-Toeller, J. Wu, S. L. Wu, Z. Yu
University of Wisconsin, Madison, WI 53706, USA

M. G. Greene, H. Neal
Yale University, New Haven, CT 06511, USA

⁵Deceased

1 INTRODUCTION

Measurements of CP -violating asymmetries in the $B^0\bar{B}^0$ system allow tests of the Standard Model by over-constraining the Unitarity Triangle through the measurement of its angles. The time-dependent CP asymmetry in a $b \rightarrow u\bar{u}d$ decay of a B^0 to a CP eigenstate allows for a direct measurement of the angle $\alpha \equiv \arg[-V_{td}V_{tb}^*/V_{ud}V_{ub}^*]$ if the decay is dominated by the tree amplitude. The contribution from penguin diagrams gives rise to a correction $\Delta\alpha = \alpha_{\text{eff}} - \alpha$ that can be inferred through an isospin analysis [1] as illustrated in Fig. 1. The theoretical error from isospin-breaking effects is typically estimated to be smaller than 10 degrees [2].

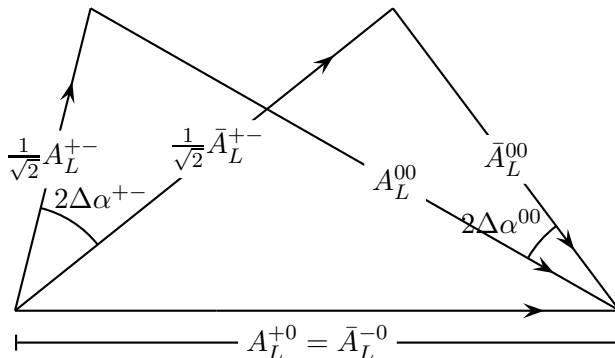


Figure 1: Isospin Triangles relating the amplitudes of the modes $B^0 \rightarrow \rho^+\rho^-$, $B^0 \rightarrow \rho^0\rho^0$, $B^+ \rightarrow \rho^+\rho^0$ and their charge conjugates for a given polarization (e.g., CP -even longitudinal polarization).

The $\pi^+\pi^-$ final state ($CP=1$) was expected to be an ideal candidate for the study of α . However, the recent measurement of $B^0 \rightarrow \pi^0\pi^0$ confirms that this mode suffers from substantial penguin contamination [3]. This severely limits the possibility of a model-independent measurement of α with currently available statistics. On the other hand, the recent experimental results shown in Table 1 confirm the theoretical expectation [4] of a smaller penguin contribution in the $\rho\rho$ system with respect to the $\pi\pi$ case (charge-conjugate decay modes are always assumed throughout this paper).

Table 1: Recent measurements of $B \rightarrow \rho\rho$ branching fractions.

Decay	BABAR	Belle
$BR(B^+ \rightarrow \rho^+\rho^0) \times 10^6$	$22.5^{+5.7}_{-5.4} \pm 5.8$ [5]	$31.7 \pm 7.1^{+3.8}_{-6.7}$ [6]
$BR(B^0 \rightarrow \rho^+\rho^-) \times 10^6$	$30 \pm 4 \pm 5$ [7]	
$BR(B^0 \rightarrow \rho^0\rho^0) \times 10^6$	< 2.1 (90 % C.L.) [5]	

In $\rho\rho$ decays the final state is not, in general, a CP eigenstate, and an isospin triangular relation holds for each of the three helicity states, which can be separated through an angular analysis. However, the measured polarizations in $\rho^+\rho^-$ and $\rho^+\rho^0$ modes indicate a dominance of the helicity 0 state (longitudinal polarization), that is, of a $CP=+1$ eigenstate. A measurement of the polarization in $B^0 \rightarrow \rho^0\rho^0$ would complete the isospin triangle, but this mode has not been

observed so far. The best present limit on the $\rho^0\rho^0$ decay was obtained by *BABAR* with a sample of 89 million $\Upsilon(4S) \rightarrow B\bar{B}$ decays [5]. The resulting Grossman–Quinn [8] bound that can be set on the penguin contribution [7, 9] is more stringent than in the $\pi\pi$ case, but knowledge of the $B^0 \rightarrow \rho^0\rho^0$ rate is still expected to be the limiting factor to the accuracy of the α measurement with $\rho\rho$ decays. In [8], Grossman and Quinn show that the angle $2\Delta\alpha^{+-}$ (see Fig. 1) between the two triangles is maximum when the two isospin triangles have opposite direction and they are right triangles. In that case, the bound takes simply the form

$$\sin^2 \Delta\alpha^{+-} \leq \frac{f_L^{00} \times \mathcal{B}(B^0 \rightarrow \rho^0\rho^0)}{f_L^{+0} \times \mathcal{B}(B^+ \rightarrow \rho^+\rho^0)} \quad (1)$$

where f_L^{00} and f_L^{+0} are the fraction of longitudinal polarization in $B^0 \rightarrow \rho^0\rho^0$ and $B^+ \rightarrow \rho^+\rho^0$ decays respectively, and $\mathcal{B}(B^0 \rightarrow \rho^0\rho^0)$ and $\mathcal{B}(B^+ \rightarrow \rho^+\rho^0)$ the respective branching fractions.

In this paper, we present a search for the $\rho^0\rho^0$ final state performed at *BABAR* on a sample of 227 million $\Upsilon(4S) \rightarrow B\bar{B}$ decays. Improvements over the previous result are achieved from the increased statistics and from optimizations of the analysis, which result in an increased sensitivity.

2 THE *BABAR* DETECTOR AND DATASET

The *BABAR* detector operates at the PEP-II asymmetric *B* Factory at SLAC and is described in detail elsewhere [10]. The data samples used in this analysis correspond to an integrated luminosity of 205.4 fb⁻¹ collected at the $\Upsilon(4S)$ resonance, and of 16.1 fb⁻¹ collected about 40 MeV below the $\Upsilon(4S)$ resonance in order to study the $q\bar{q}$ continuum background. Large samples of Monte Carlo data are also used to model signal *B* backgrounds.

3 ANALYSIS METHOD

We fully reconstruct $B^0 \rightarrow \rho^0\rho^0$ candidates from their decay products $\rho^0 \rightarrow \pi^+\pi^-$ with four charged tracks in the final state. Charged track candidates are required to originate from a single vertex near the interaction point. We select ρ^0 candidates with requirements on the $\pi^+\pi^-$ invariant mass, loose enough to retain sidebands for later fitting.

Improvements in the track reconstruction efficiency and in the understanding of the associated systematic error have allowed us to extend the accepted momentum range with respect to the previous analysis, and consequently increase the selection efficiency by 25%. The particle identification capabilities of the *BABAR* detector are used to reject tracks identified as electrons, kaons, or protons. A set of kinematic variables describing the shape of the event is used to suppress the $q\bar{q}$ continuum background. The identification of signal events is based on two kinematic variables: the beam–energy substituted mass of the *B*

$$m_{\text{ES}} = \sqrt{(s/2 + \mathbf{p}_i \cdot \mathbf{p}_B)^2 / E_i^2 - \mathbf{p}_B^2} \quad (2)$$

(where the initial four–momentum (E_i, \mathbf{p}_i) and the *B* momentum \mathbf{p}_B are defined in the laboratory frame), and the difference between the reconstructed *B* energy in the center–of–mass frame and its known value

$$\Delta E = E_B^{\text{CM}} - \sqrt{s}/2. \quad (3)$$

An unbinned extended maximum likelihood fit is then performed on the selected sample to evaluate the signal yield using several discriminating variables. The probability density functions (PDF) entering the likelihood function are built as the sum of several components that describe separately the signal, the $q\bar{q}$ continuum, and various background $B\bar{B}$ decays. The result was revealed only after the finalization and validation of the full analysis.

3.1 Angular Observables

The angular distribution of the B meson decay to a vector-vector (VV) final state is a combination of S-, P-, and D-wave contributions with unknown relative amplitudes. The helicity angles (θ_i , ϕ_i , $\phi = \phi_1 - \phi_2$, $i = 1, 2$) are defined by the direction of the two-body ρ^0 decay axis and the direction opposite the B in the ρ^0 rest system, as shown in Fig. 2.

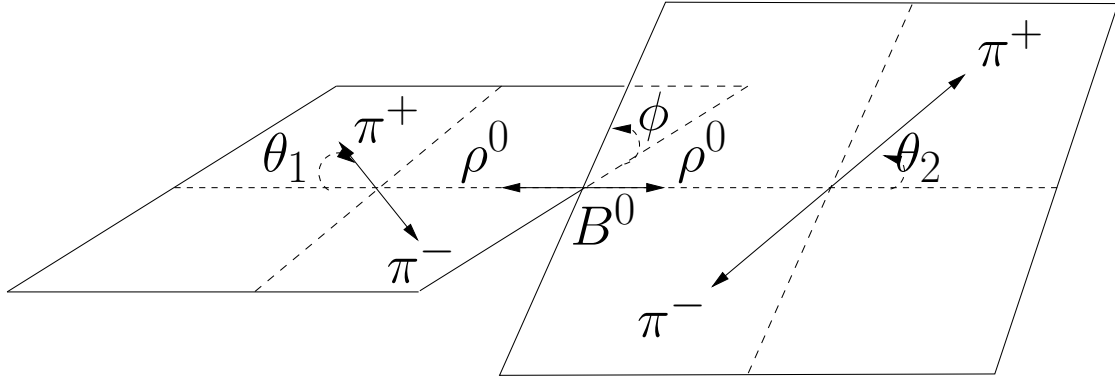


Figure 2: Definition of helicity angles θ_1 , θ_2 , and ϕ , for the decay $B^0 \rightarrow \rho^0 \rho^0$. The ρ^0 final states are shown in their rest frames.

Due to quark spin conservation, the longitudinal polarization A_L is expected to dominate the VV decays. However, this expectation might be strongly violated in penguin-dominated decays, as has been observed in $B \rightarrow \phi K^*$ [5]. Since the azimuthal angle ϕ does not provide any significant background suppression, and there are no acceptance effects for this observable, we integrate over it, which results in:

$$\frac{1}{\Gamma} \frac{d^2\Gamma}{d\cos\theta_1 d\cos\theta_2} = \frac{9}{8\pi} \left[\cos^2\theta_1 \cos^2\theta_2 f_L + \frac{1}{4} \sin^2\theta_1 \sin^2\theta_2 (1 - f_L) \right] \quad (4)$$

The two helicity observables $\mathcal{H}_i = |\cos\theta_i|$ are used in the fit to measure the longitudinal polarization of the decay, $f_L = |A_0|^2 / (|A_0|^2 + |A_{+1}|^2 + |A_{-1}|^2)$, where A_λ ($\lambda = 0, +1, -1$) correspond to the helicity amplitudes of the two ρ 's in the B rest system. These observables also provide additional background suppression. The limit on the branching fraction can be expressed as a function of f_L . The hypothesis $f_L = 1$ gives the most conservative upper limit on the A_L^{00} amplitude, shown in Fig. 1. This is also the relevant result for the measurement of α through the isospin analysis.

3.2 Event Selection

In order to reject the dominant quark-antiquark continuum background, we require $|\cos\theta_T| < 0.8$, where θ_T is the angle between the B -candidate thrust axis and that of the remaining tracks and neutral clusters in the event, calculated in the CM frame. The other event-shape discriminating variables include the polar angles of the B momentum vector and the B -candidate thrust axis with respect to the beam axis in the $\Upsilon(4S)$ frame, and the two Legendre moments L_0 and L_2 of the energy flow around the B -candidate thrust axis. These variables are combined in a neural network, which is trained using off-resonance beam data and signal Monte Carlo data. The neural network output is transformed into a Gaussian-shaped variable (called \mathcal{E} -variable hereafter), without any loss of discriminant power, to make the shape easier to fit.

To further suppress background, we use multivariate algorithms to identify the flavor of the other B in the event (tagging) [11]. The suppression power comes from the fact that signal and background have different tagging efficiencies in the various tagging categories. These categories correspond to different methods of identifying the b content of the other B meson in the event. We use five tagging categories c_{tag} (lepton, two kaon, inclusive, and the untagged event categories). Since $B\bar{B}$ events tagged by the best performing tagging categories (notably by leptons) have a lower $q\bar{q}$ background, the splitting into tagging categories improves the discrimination of the continuum.

To summarize, we use eight primary observables to characterize each event candidate: $\vec{x}_i = \{m_{\text{ES}}, \Delta E, \mathcal{E}, m(\pi^+\pi^-)_1, m(\pi^+\pi^-)_2, \mathcal{H}_1, \mathcal{H}_2, c_{\text{tag}}\}$. The ranges for the key discriminating variables are the following: we require $m_{\text{ES}} > 5.24 \text{ GeV}/c^2$ and $|\Delta E| < 85 \text{ MeV}$ (the signal m_{ES} and ΔE resolutions are $2.5 \text{ MeV}/c^2$ and 20 MeV respectively), $m(\pi^+\pi^-)_i$ between 0.55 and $1.0 \text{ GeV}/c^2$, and $\mathcal{H}_i < 0.99$. The latter cut removes a region with very low efficiency.

Additional selection criteria are finally applied to veto the most dangerous source of $B\bar{B}$ to charm background, namely $B^0 \rightarrow D^-\pi^+ \rightarrow K^+(\pi^+)\pi^-\pi^-\pi^+$, by requiring the invariant mass of the three-particle combination that excludes the highest-momentum track in the B frame to be inconsistent with a D meson.

After applying all selection criteria, the event sample has on average 1.05 candidates per event. When several candidates are selected in the same event, one candidate is selected randomly. The selection efficiency, measured on signal Monte Carlo samples, is 27% (32 %) for the longitudinally (transversely) polarized signal. This corresponds to an expected signal yield in our data sample of about 60 events for a branching fraction of 1×10^{-6} . The fraction of selected events where the four candidate tracks do not match the true event tracks, called self-cross-feed (SCF) events in the following, is 22% (8%) for longitudinal (transverse) polarization. The large self-cross-feed for longitudinal signal is due to the presence of soft pions that can be easily exchanged with soft particles from the other B .

3.3 Backgrounds

The selected sample is expected to be dominated by $q\bar{q}$ combinatorial background. However, the most dangerous backgrounds are expected to come from other B decays, in particular from final states with four charged particles that can mimic the signal in the distribution of m_{ES} and ΔE , for four-pion final states. As mentioned above, the B to charm decays are suppressed by explicit veto cuts. For the B to charmless decays, we expect contaminations from more than 50 modes, the most important ones being listed in Table 2. The mode $B^0 \rightarrow a_1^\pm \pi^\mp \rightarrow \rho^0 \pi^\pm \pi^\mp$ is an irreducible source of background. The discrimination of this mode relies mainly on the ρ mass distributions.

The other charmless modes have smaller impact on the result. The most important ones are described by specific PDFs, in order to improve the background model in the likelihood fit. We fix the yields of well measured modes ($\rho^+ \rho^0$, $\rho^+ \rho^-$, $\rho\pi$) and modes which are isospin-related to measured modes ($\rho^0 K^{*0}$), and vary these yields to evaluate the corresponding systematic error.

Table 2: Background categories which are either floated or fixed in the fit to the data sample. The yield uncertainties in the fixed background categories (both statistical and systematic) are taken into account in the evaluation of the systematic error.

Background Category	Yield
$q\bar{q}$	floated
$B \rightarrow \text{charm}$	floated
$B^0 \rightarrow a_1^\pm \pi^\mp$	floated
$B^0 \rightarrow \rho^0 K^{*0}$	$25 \pm 5 \pm 16$ [5]
$B^+ \rightarrow \rho^+ \rho^0$	$78 \pm 9 \pm 18$ [5]
$B \rightarrow \rho\pi$ modes	$34 \pm 6 \pm 4$ [12]
$B^0 \rightarrow \rho^+ \rho^-$	$14 \pm 4 \pm 3$ [7]
other charmless B decays	floated

3.4 Likelihood Fit

The signal is obtained by maximizing the extended likelihood function

$$\mathcal{L} = \exp\left(-\sum_{j=1}^{N_{\text{cat}}} n_j\right) \prod_{i=1}^{N_{\text{cand}}} \left(\sum_j n_j \mathcal{P}_j(\vec{x}_i; \vec{\beta})\right) \quad (5)$$

with several event categories j : signal (including a SCF fraction), continuum $q\bar{q}$, and several $B\bar{B}$ background categories listed in Table 2. Each $\mathcal{P}_j(\vec{x}_i; \vec{\beta})$ is the PDF for the observable \vec{x}_i , and is described by the PDF parameters $\vec{\beta}$.

The event yields n_j in different categories are obtained by minimizing the quantity $-2 \ln \mathcal{L}$. The statistical significance of a signal is defined as the square root of the change in $-2 \ln \mathcal{L}$ when constraining the number of signal events to zero in the likelihood fit. The assumption of negligible correlations among most of the fit input variables has been validated with MC simulation and data. However, there are effects which do introduce noticeable correlations in the samples of signal and background events, such as helicity angles correlation in signal, and mass-helicity correlation in background, as discussed below.

3.5 PDF Parameterization

We use double-Gaussian functions to parameterize the ΔE and m_{ES} PDF's for signal, and a relativistic P-wave Breit-Wigner convoluted with a Gaussian resolution function for the resonance masses. The \mathcal{E} -variable is described by an asymmetric Gaussian plus a single Gaussian function for both signal and background. The signal helicity PDF is expressed as a function of the longitudinal polarization (see Eq. 4). The ideal angular distribution is multiplied by the detector acceptance function $\mathcal{G}(\mathcal{H}_1, \mathcal{H}_2)$. We obtain the acceptance function from a fit to a sample of MC events with transverse and longitudinal polarization.

For the combinatorial background we use low-degree polynomials for ΔE and resonance masses, and an empirical phase-space function for m_{ES} (known as Argus function [13]):

$$f(x) \propto x\sqrt{1-x^2} \exp[-\xi(1-x^2)] , \quad (6)$$

where $x = m_{\text{ES}}/E_{\text{beam}}$, and ξ is a parameter measuring the curvature of the distribution near the end-point. The background parameterization of resonance masses also includes a resonant component to account for resonance production, which is described by the same P-wave Breit-Wigner function used for the signal ρ shape. The background helicity-angle distribution is separated into contributions from combinatorial background and from resonances. The resonances are assumed to be unpolarized. We parameterize the combinatorial helicity distribution with a second-degree polynomial and an exponential function to allow for the increased fraction of fake ρ candidates with low momentum pions near $\mathcal{H}_i = 1$. The amount of peaking near $\mathcal{H}_i = 1$ depends on the ρ candidate mass and is parameterized accordingly. Fig. 3 shows the m_{ES} , ΔE , and \mathcal{E} PDFs for combinatorial background and longitudinal signal. The two-dimensional mass-helicity distribution for combinatorial background, and the projection of the helicity distribution for longitudinal signal are also shown.

The PDFs for exclusive B decay modes are modeled with non-parametric distributions describing the shapes of the observables, except when certain distributions are expected to be identical to those used for signal. These distributions are described by smoothed histograms [14] with a large number of bins. In the B -background modes the two ρ^0 candidates can have very different mass and helicity distributions. This happens, for example, when one of the two ρ^0 s is real (e.g. $\rho^+\rho^0$, ρ^0K^{*0}) or when only one of the two ρ^0 s contains a hard bachelor pion ($a_1\pi$). In such cases, we consider a four-variable correlated mass/helicity PDF. The inclusive B -to-charm and B -to-charmless categories are parameterized similarly to the exclusive modes, they include the remaining B decay modes not modeled explicitly, and their yield is left free in the fit, to include possible unaccounted background sources and compensate for possible imperfections in the background model.

The B -flavor tagging PDFs for signal and background are simply the discrete distributions of tagging efficiencies. Large samples of fully reconstructed B meson decays are used to obtain the B -tagging efficiencies for signal B decays and to control the MC values of B -tagging efficiencies for the B backgrounds. Continuum background efficiencies are obtained from the sideband data.

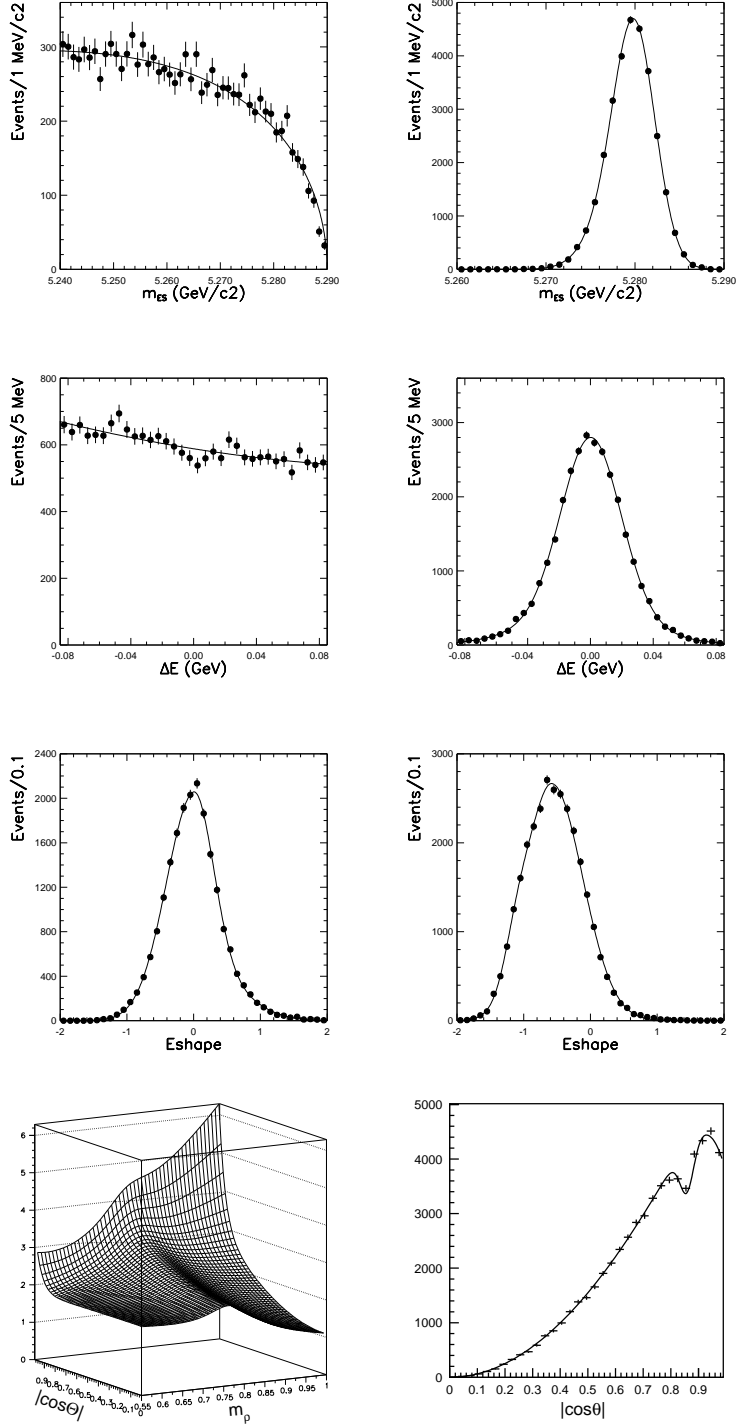


Figure 3: PDFs of the observables (from top to bottom): m_{ES} , ΔE , and \mathcal{E} , for combinatorial background (left) and longitudinal signal (right). The bottom row shows the combinatorial background mass-helicity two-dimensional PDF (left), and the projection of the helicity distribution for signal (right). The small dip near $|\cos\theta| = 0.85$ is due to the D -veto acceptance effect.

4 PHYSICS RESULTS

Table 3 shows the results of the fit. No significant yield is observed, and an upper limit on the branching fraction of $B^0 \rightarrow \rho^0 \rho^0$ is set. As mentioned earlier, 100% longitudinally polarized signal is used in the fit, as it was checked that it gives the most conservative estimate for the upper limit.

Table 3: Results of the fit: Signal yield (N_S), selection efficiency (Eff), branching fraction (\mathcal{B}), upper limit at 90% confidence level (U.L.) and significance of the measurement, defined as $\sqrt{\Delta(-2 \ln \mathcal{L})}$ when constraining the number of signal events to zero in the fit. The first error corresponds to the statistical uncertainty and the second one to the systematic uncertainty, discussed in next section.

Quantity	Value
N_S	$33_{-20}^{+22} \pm 12$
Eff (%)	27.1 ± 1.3
$\mathcal{B}(\times 10^{-6})$	$0.54_{-0.32}^{+0.36} \pm 0.19$
U.L. ($\times 10^{-6}$)	1.1 (1.0 statistical only)
Significance ($\sqrt{\Delta(-2 \ln \mathcal{L})}$)	1.6 (1.9 statistical only)

Figure 4 shows the result of the fit projected onto the m_{ES} and ΔE observables. The histograms show the data after a cut on the quantity $\mathcal{P}_{\text{sig}}/(\mathcal{P}_{\text{sig}} + \mathcal{P}_{\text{back}})$ has been applied, where \mathcal{P}_{sig} and $\mathcal{P}_{\text{back}}$ are the probabilities for a given event to be signal and background respectively, and are evaluated using all the observables except the one that is being plotted. The cut is optimized for each variable separately. The solid (dashed) line shows the projection for the full fit (background only) after the same cut is applied.

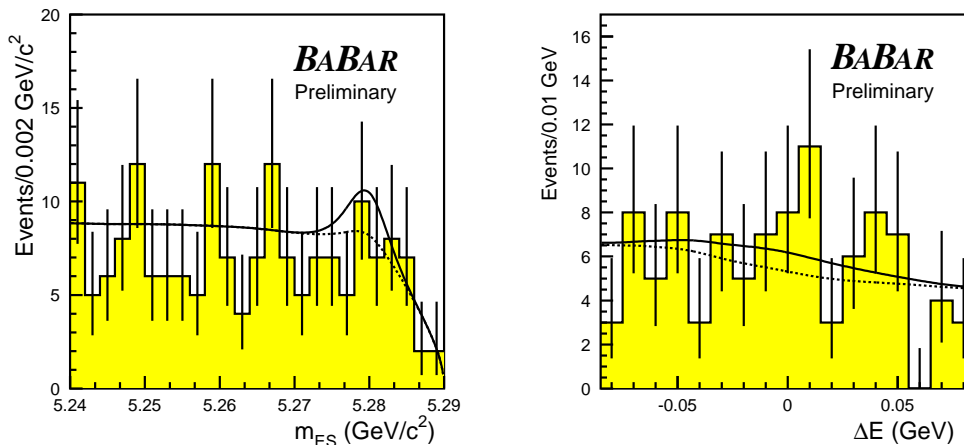


Figure 4: Fit result projections onto m_{ES} and ΔE . The histograms correspond to the data and the solid (dashed) line to the full (background only) fit after a cut on the quantity $\mathcal{P}_{\text{sig}}/(\mathcal{P}_{\text{sig}} + \mathcal{P}_{\text{back}})$ is applied. The projections contain 22.5% and 23.9% of signal, and less than 0.5% and 0.2% of continuum background respectively.

5 SYSTEMATIC STUDIES

Table 4 summarizes the systematic errors on the branching fraction. We include the uncertainty in the total number of B mesons, the uncertainties coming from selection cuts, such as track multiplicity, thrust angle, and vertex requirements, and the uncertainty in particle identification. The uncertainty on the selection efficiency is estimated from Monte Carlo and is dominated by the reconstruction of soft tracks. The accuracy of the simulation of the key observables m_{ES} and ΔE is estimated using the $B^0 \rightarrow D^- \pi^+ \rightarrow K^+ \pi^- \pi^- \pi^+$ control sample.

The peaking $B\bar{B}$ background has been taken into account in the fit with three fixed components. The effect of their systematic uncertainty on the signal is evaluated by adding to the data known samples of background Monte Carlo events and observing the variation of the result.

Monte Carlo studies show that the interference between signal and $a_1^\pm \pi^\mp$ may not be neglected and could significantly bias the measurement. Assuming for the branching fraction of the two modes the central values measured without accounting for interference, and accounting for acceptance and likelihood fit, the systematic bias is estimated at the level of 7.5 events.

To obtain the error associated to the uncertainty in the PDFs parameters, 200 Monte Carlo experiments are performed with the parameters varied within their errors. The width of the fitted yield distribution is taken as systematic error. Finally, we assign a systematic error of ± 3 events to cover a possible fit bias evaluated with Monte Carlo experiments.

Table 4: Summary of systematic errors in the measurement of the $B^0 \rightarrow \rho^0 \rho^0$ branching fraction.

Source	Uncertainty	
	Yield fraction	Number of events
Multiplicative		
Number of B mesons	1.1%	0.4
Track multiplicity cut	1%	0.3
Thrust angle cut	1%	0.3
Vertex requirement	2%	0.7
PID cut	2%	0.7
Track finding	3.2%	1.1
MC statistics	<1%	<0.3
Additive		
B background	17.4%	5.8
$a_1\pi$ interference	22.5%	7.5
PDF variation	18%	6.0
Fit bias	9%	3.0
Total	35%	11.7

Taking systematic uncertainties into account, the measured value for the $B \rightarrow \rho^0 \rho^0$ branching fraction is

$$\mathcal{B}(B \rightarrow \rho^0 \rho^0) = (0.54_{-0.32}^{+0.36} \pm 0.19) \times 10^{-6}$$

or an upper limit of 1.1×10^{-6} at 90% confidence level.

6 SUMMARY

With a sample of 227 million $\Upsilon(4S) \rightarrow B\bar{B}$ decays collected with the *BABAR* detector we have searched for the decay mode $B^0 \rightarrow \rho^0\rho^0$. We set an upper limit of 1.1×10^{-6} (90% C.L.) on the branching fraction of this decay mode. Our results are preliminary. This result has important implications for understanding the penguin contribution and constraints on the CKM angle α with the $B \rightarrow \rho\rho$ decays. With the $B^0 \rightarrow \rho^+\rho^-$ values of the branching fraction and longitudinal polarization [7], the measured $B^0 \rightarrow \rho^+\rho^-$ S and C CP -violating time-dependent asymmetry parameters [15], the $B^+ \rightarrow \rho^+\rho^0$ values of the branching fraction and longitudinal polarization [5] [6] [12], and the measured branching ratio of $B^0 \rightarrow \rho^0\rho^0$ measured in this analysis, neglecting electroweak penguins, non-resonant and $I = 1$ isospin contributions, and using isospin analysis [15], we obtain a new value for α :

$$\alpha = (96 \pm 10(\text{stat}) \pm 4(\text{syst}) \pm 11(\text{penguin}))^\circ$$

To extract alpha a χ^2 in which all the measured quantities and the angles $2\Delta\alpha^{+-}$ and $2\Delta\alpha^{00}$ of Fig. 1 are expressed as a function of the length of the two isospin triangles' sides is minimized. The confidence level on α is obtained by a scan of the difference between $\chi^2(\alpha)$ for a given value of α and the minimum of this χ^2 . Fig. 5 presents the result of this scan.

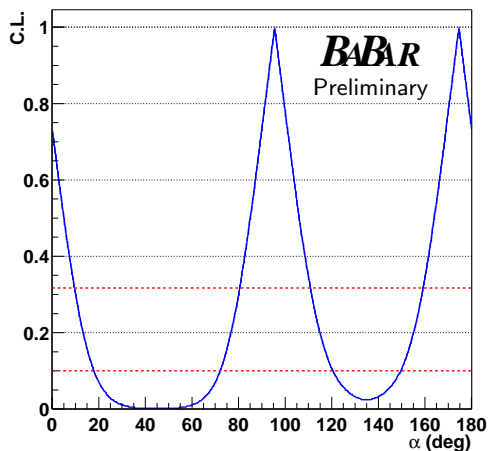


Figure 5: Confidence Level on α obtained from the measured branching fraction, fraction of longitudinal polarization, and CP parameters of $B^0 \rightarrow \rho^+\rho^-$, branching fraction and fraction of longitudinal polarization of $B^+ \rightarrow \rho^+\rho^0$, and the $B^0 \rightarrow \rho^0\rho^0$ branching fraction measurement from this analysis, using isospin analysis. The dashed lines correspond to the 68% (top) and 90% (bottom) confidence intervals.

7 ACKNOWLEDGMENTS

We are grateful for the extraordinary contributions of our PEP-II colleagues in achieving the excellent luminosity and machine conditions that have made this work possible. The success of

this project also relies critically on the expertise and dedication of the computing organizations that support *BABAR*. The collaborating institutions wish to thank SLAC for its support and the kind hospitality extended to them. This work is supported by the US Department of Energy and National Science Foundation, the Natural Sciences and Engineering Research Council (Canada), Institute of High Energy Physics (China), the Commissariat à l’Energie Atomique and Institut National de Physique Nucléaire et de Physique des Particules (France), the Bundesministerium für Bildung und Forschung and Deutsche Forschungsgemeinschaft (Germany), the Istituto Nazionale di Fisica Nucleare (Italy), the Foundation for Fundamental Research on Matter (The Netherlands), the Research Council of Norway, the Ministry of Science and Technology of the Russian Federation, and the Particle Physics and Astronomy Research Council (United Kingdom). Individuals have received support from CONACyT (Mexico), the A. P. Sloan Foundation, the Research Corporation, and the Alexander von Humboldt Foundation.

References

- [1] M. Gronau and D. London, Phys. Rev. Lett. **65**, 3381 (1990).
- [2] See *e.g.*, M. Ciuchini, talk at CKM Angles and *BABAR* Planning Workshop, SLAC October 3, 2003.
- [3] B. Aubert *et al.* [*BABAR* Collaboration], Phys. Rev. Lett. **91**, 241801 (2003).
- [4] R. Aleksan *et al.*, Phys. Lett. B **356**, 95 (1995).
- [5] B. Aubert *et al.* [*BABAR* Collaboration], Phys. Rev. Lett. **91**, 171802 (2003).
- [6] J. Zhang *et al.* [Belle Collaboration], Phys. Rev. Lett. **91**, 221801 (2003).
- [7] B. Aubert *et al.* [*BABAR* Collaboration], Phys. Rev. D **69**, 031102 (2004); arXiv:hep-ex/0404029, submitted to Phys. Rev. Lett.
- [8] Y. Grossman and H. R. Quinn, Phys. Rev. D **58**, 017504 (1998).
- [9] A.F. Falk *et al.*, Phys. Rev. D **69**, 011502 (2004).
- [10] B. Aubert *et al.* [*BABAR* Collaboration], Nucl. Instrum. Methods **A479**, 1 (2002).
- [11] B. Aubert *et al.* [*BABAR* Collaboration], Phys. Rev. Lett. **89**, 201802 (2003).
- [12] See tables at <http://www.slac.stanford.edu/xorg/hfag/rare/prewinter04/charmless/index.html>.
- [13] H. Albrecht *et al.* [ARGUS Collaboration], Z. Phys. C **48**, 543 (1990).
- [14] K.S. Cranmer, Comput. Phys. Commun. **136**, 198 (2001).
- [15] See *e.g.*, L. Roos talk at Rencontres de Moriond, La Thuile (Italy), March 2004, arXiv:hep-ex/0407051.